AIAA JOURNAL
Vol. 34, No. 3, March 1996

Viscoelastic Material Response with a Fractional-Derivative Constitutive Model

William P. Baker,* Lloyd B. Eldred,† and Anthony N. Palazotto‡
U.S. Air Force Institute of Technology, Wright–Patterson Air Force Base, Ohio 45433

A rubber coupon is modeled as a viscoelastic material by a fractional-derivative constitutive law to capture the material behavior over a broad frequency range. The coupon, of finite length, is clamped at one end and subject to either a forced loading or a deflection at the other end. The physical response profile of the material for this distributed model is examined in terms of a relaxation response, associated with a branch-cut integration, and a modal response.

Introduction

VISCOELASTIC materials have applications in a variety of mechanical processes, from passive damping to tire construction. Our research interest is in the response of materials used in the manufacture of aircraft tires. Such materials are forced over a broad frequency range because of changes in temperature and tire rolling velocities. A constitutive model, introduced by Bagley and Torvik,[1,2] involving fractional derivatives, seems to capture the material behavior over a substantial range in frequency.[3] We examine the behavior of a viscoelastic coupon, modeled by a fractional-derivative constitutive relationship. The coupon is clamped at one end and subject to either force loading or deflection at the other end. The response profile of this distributed model is examined in the frequency domain, and dominant features are determined.

We begin by describing the fractional-derivative constitutive relationship for rubber like materials. Then we characterize, by an integro-partial-differential equation, an experiment performed on the material to determine its viscoelastic properties. We solve the equation in the frequency domain and examine the transfer function for dominant behavior in the time domain. The material response is then calculated for a range of periodic inputs.

Viscoelastic Materials

Viscoelastic behavior occurs in a wide range of materials that show some sort of liquid-like elastic behavior. Such materials include acrylics, rubber, and glass. A conventional Hooke's-law linear elastic constitutive relationship is an inadequate representation of such viscoelastic material behaviors as stress relaxation over short and long time scales. Further, the material behavior is dependent on its own time history; that is, it has memory. Thus we wish to use a constitutive relation that provides a high degree of fidelity over a broad range of frequencies. Although higher-order polynomial differential operators could be used, they do not properly characterize the memory in the material.

A simple fractional-order-derivative[1] Kelvin–Voigt-style constitutive relationship is given by

$$\sigma = \tilde{\mathcal{D}}(\epsilon) \equiv q_0\epsilon + q_1 \frac{\partial^\alpha}{\partial t^\alpha}\epsilon \tag{1}$$

where σ and ϵ are, respectively, the stress and strain distributions within the coupon as a function of time t. Further, $\partial^\alpha/\partial t^\alpha$ is the Riemann–Liouville fractional-order derivative[4] defined as

$$\frac{\partial^\alpha}{\partial t^\alpha}x(t) = \frac{1}{\Gamma(1-\alpha)}\frac{\partial}{\partial t}\int_0^t \frac{x(\tau)}{(t-\tau)^\alpha}\,d\tau, \qquad 0 < \alpha < 1 \tag{2}$$

where $\Gamma(\cdot)$ is the gamma function. This integrodifferential operator has fading or algebraically decaying memory because of the convolution with $t^{-\alpha}$. Here we say the system has perfect memory if $\alpha = 0$ and no memory if $\alpha = 1$. Additionally, unlike the standard ($\alpha = 1$) Kelvin–Voigt model, the fractional derivative carries added stiffness into the system. This fractional-derivative model (1) was very successful at fitting experimentally measured data from rubber-like material[3] used in tire manufacturing. The creep compliance and relaxation modulus for this fractional-calculus Kelvin–Voigt model as well as the fractional-calculus Maxwell model were examined by Koeller.[5] Padovan et al.[6,7] studied the asymptotic behavior of a general class of fractional-derivative constitutive relations.

Differential Equation

An integro-partial-differential equation is developed to model a homogeneous viscoelastic experimental coupon that undergoes time-dependent longitudinal loading at a variety of frequencies. Following a standard balance of forces[8] for the uniaxially loaded isotropic coupon (see Fig. 1) and neglecting any gravity effects, one arrives at the equation

$$\rho A(x,t)\frac{\partial^2 u}{\partial t^2} = \frac{\partial}{\partial x}\left[A(x,t)\tilde{\mathcal{D}}\left(\frac{\partial u}{\partial x}\right)\right] \tag{3}$$

where ρ is the material mass density, u the element deflection from a neutral or unloaded position in the x coordinate direction, and $A(x,t)$ the local cross-sectional area of the coupon. The generic viscoelastic operator $\tilde{\mathcal{D}}$ is the differential operator defined in Eq. (1). For this analysis we will assume the cross-sectional area remains constant at A_0.

The experiment this equation models has one end of the coupon stationary while the other end is excited by the test apparatus. Thus, the corresponding boundary conditions are

$$u(0,t) = 0 \qquad \text{and} \qquad u(l,t) = \tilde{d}(t) \tag{4}$$

where l is the unloaded coupon length and $\tilde{d}(t)$ is a bounded enforced tip displacement function. When a force condition is used at the tip

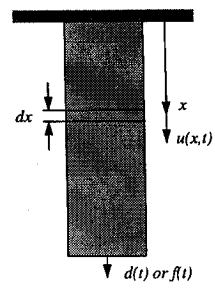

Fig. 1 Coupon experiment and description of variables.

Received Dec. 7, 1994; revision received Oct. 1, 1995; accepted for publication Nov. 16, 1995. This paper is declared a work of the U.S. Government and is not subject to copyright protection in the United States.

*Associate Professor of Mathematics.
†National Research Council Research Associate. Member AIAA.
‡Professor of Aerospace Engineering. Associate Fellow AIAA.

instead of the displacement condition, we are led to the boundary conditions

$$u(0,t)=0 \qquad \text{and} \qquad A_0\tilde{\mathcal{D}}\left(\frac{\partial u}{\partial x}(l,t)\right)=\tilde{f}(t) \tag{5}$$

where $\tilde{f}(t)$ is a bounded tip force. Finally, we imposed quiescent initial conditions.

Next, we nondimensionalize the differential equation by introducing the dimensionless variables $\xi = x/l$ and $\tau = t/T$, where l is the natural length of the undisturbed coupon and $T=\sqrt{(\rho/q_0)}l$ is the time required for a compressional wave to travel the length of a coupon of density ρ and Young's modulus q_0. We further define the new dependent variable $w(\xi,\tau)=u(l\xi,T\tau)/l$ and reduce Eq. (3) along with boundary conditions (4) or (5) to

$$\frac{\partial^2 w}{\partial \tau^2}=\frac{\partial^2}{\partial \xi^2}\mathcal{D}(w) \tag{6}$$

with displaced boundary conditions

$$w(0,\tau)=0 \qquad \text{and} \qquad w(1,\tau)=d(\tau)\equiv(1/l)\tilde{d}(T\tau) \tag{7}$$

or forced boundary conditions

$$w(0,\tau)=0 \qquad \text{and} \qquad \mathcal{D}\frac{\partial w}{\partial \xi}(1,\tau)=f(\tau)\equiv\frac{1}{A_0q_0}\tilde{f}(T\tau) \tag{8}$$

Here, the scale A_0q_0 can be thought of as the amount of force required to produce one unit of strain in an elastic medium with Young's modulus q_0. The viscoelastic differential operator has been replaced by

$$\mathcal{D}=1+\mu\frac{\partial^\alpha}{\partial \tau^\alpha} \tag{9}$$

which is the nondimensional version of Eq. (1) with $\mu = q_1/(q_0^{1-\alpha/2}\rho^{\alpha/2}l^\alpha)$.

Introducing the Laplace transform and defining the normalized displacement in the transform domain as

$$W(\xi,s)=\int_0^\infty e^{-s\tau}w(\xi,\tau)\,d\tau \tag{10}$$

the partial differential equation (6) is reduced to an ordinary differential equation.[9] The transformed equation along with the accompanying boundary conditions are solved to produce the following solutions:

Displaced boundary condition:

$$W_D(\xi,s)=\frac{\sinh\lambda(s)\xi}{\sinh\lambda(s)}D(s) \tag{11}$$

Forced boundary condition:

$$W_F(\xi,s)=\frac{\sinh\lambda(s)\xi}{\cosh\lambda(s)}\frac{\lambda^2(s)}{s^2}F(s) \tag{12}$$

where $D(s)$ and $F(s)$ are, respectively, the Laplace transform of $d(\tau)$ and $f(\tau)$, and $\lambda(s)$ is given by

$$\lambda(s)=\frac{s}{\sqrt{1+\mu s^\alpha}} \tag{13}$$

At this point, we observe that the response in the coupon due to a force $f(\tau)$ is identical to the response due to a displacement $d(\tau)$ when the force and displacement functions are related (through the Laplace transform) by

$$D(s)=\frac{\lambda^2(s)}{s^2}[\tanh\lambda(s)]F(s) \tag{14}$$

That is, a displacement schedule $d(\tau)=(g*f)(\tau)$, where

$$g(\tau)=\mathcal{L}^{-1}\left\{\frac{\tanh\lambda(s)}{1+\mu s^\alpha}\right\}(\tau) \tag{15}$$

will produce the same response as a forcing schedule $f(\tau)$. For this reason, it is sufficient to restrict our attention to analyzing the coupon's response to a displacement schedule.

Analysis of Solutions

The solution to Eq. (6) for a displacement schedule $d(\tau)$ is given by

$$w(\xi,\tau)=\int_0^\tau h(\xi,\eta)d(\tau-\eta)\,d\eta \tag{16}$$

where $h(\xi,\tau)=\mathcal{L}^{-1}\{H(\xi,s)\}(\tau)$ with the system transfer function

$$H(\xi,s)=\frac{\sinh\lambda(s)\xi}{\sinh\lambda(s)} \tag{17}$$

Knowledge of this transfer function is sufficient to characterize the coupon's behavior. Inverting the Laplace transform, we find that $h(\xi,\tau)$ can be represented as the sum of two functions: a pole contribution $h_p(\xi,\tau)$ and a branch-cut contribution $h_b(\xi,\tau)$.

The pole contribution function $h_p(\xi,\tau)$ characterizes the material behavior at early times and as such dominates the more moderate and high-frequency effects. In the complex s plane, the poles of Eq. (17) are found as roots of

$$s^2+\mu(k\pi)^2s^\alpha+(k\pi)^2=0, \qquad k=1,2,3,\ldots \tag{18}$$

We note that for each k, the roots appear in complex conjugate pairs on the principal branch, $-\pi < \arg s \le \pi$. Thus, we have the infinite set of complex roots $s_k=-\gamma_k+j\Gamma_k$, where γ_k and Γ_k represent respectively the damping coefficient and the damped natural frequency of the kth mode. In Table 1 we give the first 10 values of γ and Γ for the rubberlike material, using the parameters determined by Eldred et al.[3] for which $\alpha=0.6442$ and $\mu=0.3751$.

Applying the residue theorem,[10] we find that the pole contribution h_p produces

$$h_p(\xi,\tau)=2\sum_{k=1}^\infty\frac{(-1)^{k+1}}{r_k}e^{-\gamma_k\tau}\sin(k\pi\xi)\sin(\Gamma_k\tau-\theta_k) \tag{19}$$

where r_k and θ_k are defined by

$$\frac{d}{ds}\lambda(s)\bigg|_{s=s_k}\equiv\lambda_k=r_ke^{j\theta_k} \tag{20}$$

As $k\to\infty$, the poles can be approximated asymptotically by

$$s_k\sim k\pi\left(\nu_k-\frac{1}{(2-\alpha)\nu_k}-\frac{1+\alpha}{2(2-\alpha)^2\nu_k^3}\right) \qquad \text{with} \qquad \nu_k=[-\mu(k\pi)^\alpha]^{1/(2-\alpha)} \tag{21}$$

So for k sufficiently large (when $|\nu_k|>2.5$ the relative error is less than 5%), the damping coefficient and damped natural frequency for each mode can be approximated by

$$\gamma_k\sim[\mu(k\pi)^2]^{1/(2-\alpha)}\cos[(1-\alpha)\pi/(2-\alpha)] \qquad \text{and} \qquad \Gamma_k\sim[\mu(k\pi)^2]^{1/(2-\alpha)}\sin[\pi/(2-\alpha)] \tag{22}$$

This would lead to a damping ratio ζ and undamped natural frequency ω_n for each mode given by

$$\zeta\sim\cos[(1-\alpha)\pi/(2-\alpha)] \qquad \text{and} \qquad \omega_n\sim[\mu(k\pi)^2]^{1/(2-\alpha)} \quad \text{as} \quad k\to\infty \tag{23}$$

Table 1 Pole locations for rubberlike material

k	Damping, γ_k	Frequency, Γ_k	$\log_{10}\Gamma_k$	Time constant, $1/\gamma_k$
1	1.10	3.79	0.579	0.910
2	3.49	8.37	0.923	0.286
3	6.84	13.60	1.133	0.146
4	10.98	19.42	1.288	0.091
5	15.79	25.80	1.411	0.063
6	21.19	32.69	1.514	0.047
7	27.13	40.06	1.603	0.037
8	33.55	47.88	1.680	0.030
9	40.42	56.13	1.749	0.025
10	47.71	64.79	1.812	0.021

respectively. Because the time constant $1/\gamma_k$ (see Table 1) for each mode is $\mathcal{O}(k^{-2/(2-\alpha)})$, only higher-order modes contribute on this very short time scale.

On the other hand, the branch-cut contribution h_b is given by

$$h_b(\xi, \tau) = \frac{1}{\pi} \int_0^\infty e^{-r\tau} H_I(\xi, r)\, dr \tag{24}$$

with

$$H_I(\xi, r) = \operatorname{Im} H(\xi, re^{j\pi}) \tag{25}$$

where Im means the imaginary part, and the branch cut is taken to lie along the negative real axis. This contribution characterizes the relaxation behavior which takes place over a very long time and is therefore a very low-frequency effect. The effect of the branch-cut contribution as $\tau \to \infty$ is found by applying Watson's lemma[11] to Eq. (24). This produces

$$h_b(\xi, \tau) \sim \frac{\Gamma(3+\alpha)}{6} \frac{\xi(1-\xi^2)}{\tau^{3+\alpha}} \mu \sin \alpha\pi \qquad \text{as} \qquad \tau \to \infty \tag{26}$$

This illustrates the long-time relaxation behavior of the transfer function, where we see that the strength diminishes algebraically as $\mathcal{O}(\tau^{-(3+\alpha)})$. Thus, in the long-time limit, the algebraic decay of h_b can be expected to dominate the exponential decay of h_p. We also note that $\sin \alpha\pi$ vanishes as α approaches 1, that is, the branch-cut contribution vanishes. This is indicative of the standard Kelvin–Voigt model with integer-order derivatives. Such a constitutive law has no branch-cut contribution, and all of the relaxation behavior is expressed in terms of nonoscillatory, exponentially decaying functions, whereas the fractional calculus law ($\alpha \neq 1$) contains algebraic decay as well as oscillatory exponential decay.

To see the relative significance of pole contributions, we examine in the frequency domain a plot of $|H(\xi, j\omega)|$ and compare that with $|H_p(\xi, j\omega)|$, which represents only the pole contributions to the transfer function. Figure 2 shows a plot of $|H(\xi, j\omega)|$ over three decades in frequency, from 0.1 to 100 Hz (plotted as the logarithm to base 10), and for $0 \leq \xi \leq 1$. Here again we use $\alpha = 0.6442$ and $\mu = 0.3751$; this closely approximates the rubberlike material modeled by Eldred et al.[3] From the plot we see a linear growth at the low-frequency end as ξ ranges from 0 to 1. This is the expected behavior, as can be seen from Eqs. (13) and (17) as $s \to 0$. At approximately 0.6 on the log frequency axis (3.8 Hz), we see a major deviation from the linear behavior at low frequency. This corresponds to the first mode associated with $h_p(\xi, \tau)$ (the first pole contribution). The next mode occurs at approximately 0.9 (8.4 Hz), which compares well with Table 1. Higher-order modes do not appear as dominate because of the strength of the damping coefficients. In Fig. 3, we plot $|H_p(\xi, j\omega)|$ associated with the pole contribution only. Here we compute the function based on only the first 200 poles. This, of course, leads to a Gibbs phenomenon at $\xi = 1$. To mitigate the effect, we introduced the linear low-frequency behavior ξ and removed its Fourier series representation. This produces

$$H_p(\xi, j\omega) = \xi + 2 \sum_{k=1}^{\infty} \frac{(-1)^k}{r_k^2} \sin(k\pi\xi) \times \left(\frac{j\omega \operatorname{Im} \lambda_k - \operatorname{Im} s_k \lambda_k}{\omega^2 + 2j\omega \operatorname{Re} s_k - |s_k|^2} - \frac{r_k^2}{k\pi} \right) \tag{27}$$

with λ_k defined by Eq. (20) and s_k a root of Eq. (18). Examining Fig. 3, we see the pole contribution alone appears to retain most of the dominant features of the transfer function. In Fig. 4, we plot $|H(\xi, j\omega) - H_p(\xi, j\omega)|$, taking into consideration potential phase error. (The reader should observe the scale change between the vertical axis of Figs. 2 and 3 and that of Fig. 4.) Here we see that the greatest errors take place near the low-frequency end and near $\xi = 1$. Thus, the effect of $h_b(\xi, \tau)$ on the solution of Eq. (6) depends highly on the frequency content of the forcing function and the location along the coupon. If the forcing contains a large low-frequency component or the response is sampled near $\xi = 1$, then $h_b(\xi, \tau)$ has a strong influence on the solution. If, on the other hand, the forcing is dominated by high-frequency components and the response is sampled away from $\xi = 1$, then the branch-cut portion of the transfer function is less significant, and it is sufficient to characterize the response by $h_p(\xi, \tau)$ only. To illustrate this feature, we examine the response of the system to a tip displacement function

$$d(\tau) = d_0 \sin \omega_0 \tau \tag{28}$$

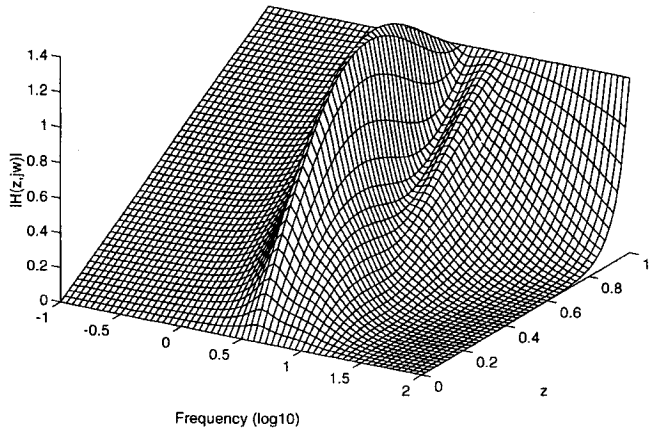

Fig. 2 Magnitude of the transfer function in the space and frequency domains.

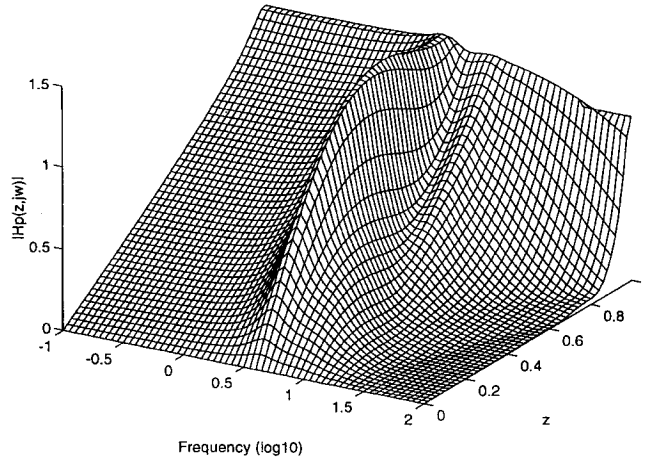

Fig. 3 Magnitude of the poles-only transfer function in the space and frequency domains.

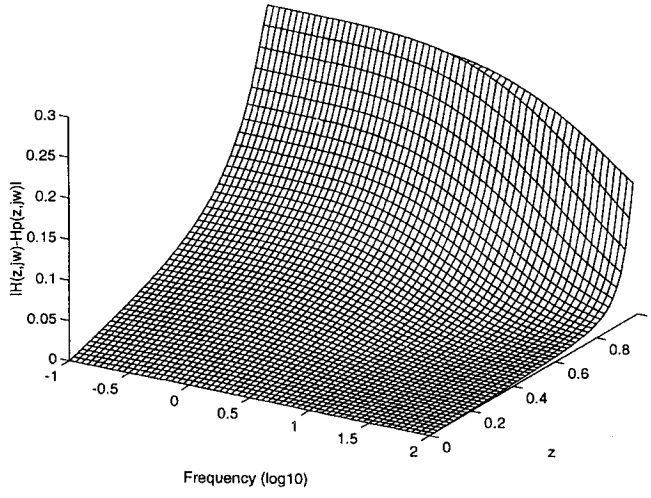

Fig. 4 Absolute error between the transfer function (branch cut) and the poles-only transfer function.

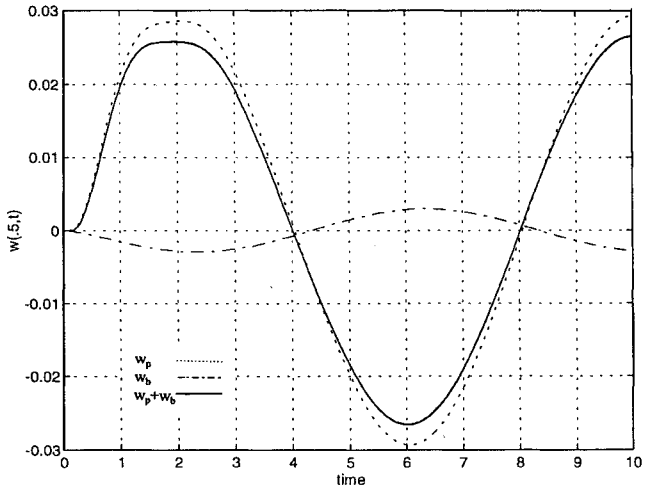

Fig. 5 Time-domain plot of the displacement at $\xi = 0.5$ for a low excitation frequency, $\omega_0 = \pi/4$, comparing the poles-only response, the branch-cut-only response, and the total response.

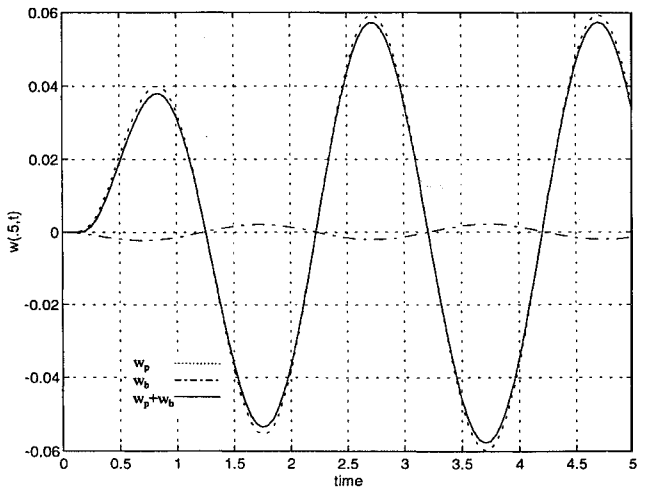

Fig. 6 Time-domain plot of the displacement at $\xi = 0.5$ for a moderate excitation frequency, $\omega_0 = \pi$, comparing the poles-only response, the branch-cut-only response, and the total response.

where d_0 is a fraction of the coupon length and ω_0 is the excitation frequency. Using Eq. (16) for each portion of the transfer function (i.e., h_p and h_b), we obtain the responses $w_p(\xi, t)$ and $w_b(\xi, t)$. The pole contribution w_p has the form

$$w_p(\xi, t) = d_0 \sum_{k=1}^{\infty} \frac{(-1)^{k+1}}{r_k} A_k(t; \omega_0) \sin(k\pi\xi) \tag{29}$$

where

$$A_k(t; \omega_0) = e^{-\gamma_k t} \sin(\delta_k^-) \sin\left(\Gamma_k t - \theta_k + \delta_k^+\right) - \sin\left(\theta_k - \delta_k^-\right) \sin\left(\omega_0 t - \delta_k^+\right) \tag{30}$$

with θ_k given by Eq. (20) and

$$\delta_k^{\pm} = \frac{1}{2}\left[\arctan\left(\frac{\Gamma_k + \omega_0}{\gamma_k}\right) \pm \arctan\left(\frac{\Gamma_k - \omega_0}{\gamma_k}\right)\right] \tag{31}$$

Likewise, we find the branch-cut contribution w_b has the form

$$w_b(\xi, t) = d_0 B(\xi; \omega_0) \sin[\omega_0 t + \beta(\xi; \omega_0)] + d_0 C(\xi, t; \omega_0) \tag{32}$$

where $B(\xi; \omega_0)$ and $\beta(\xi; \omega_0)$ are respectively the modulus and phase function of

$$\frac{1}{\pi} \int_0^{\infty} \frac{H_I(\xi, r)}{r + j\omega_0} \, dr \tag{33}$$

and

$$C(\xi, t; \omega_0) = \frac{\omega_0}{\pi} \int_0^{\infty} e^{-rt} \frac{H_I(\xi, r)}{r^2 + \omega_0^2} \, dr \tag{34}$$

with H_I given by Eq. (25). Figures 5, 6, and 7 depict the material response at $\xi = 0.5$ due to excitation frequencies $\omega_0 = \pi/4, \pi$, and 3π, respectively. These frequencies represent low, moderate, and high frequencies based on the relative time scales of the excitation period $(2\pi/\omega_0)$ and the time constant for the first mode $(1/\gamma_1)$. In each figure we plot the displacement due to the pole contribution $w_p(\xi, \tau)$, the branch-cut contribution $w_b(\xi, \tau)$, and the total displacement (both pole and branch-cut contributions), $w(\xi, \tau)$. Here $w(\xi, \tau)$ is found by numerically inverting the Laplace transform. In each case, we see the majority of the response can be accounted for by the pole contribution. However, as the frequency diminishes, the significants of the branch-cut becomes more apparent. The relative error in amplitude (the ratio of maximum w_b amplitude to maximum w_p amplitude) can be seen to increase as the frequency decreases. For frequencies $\pi/4, \pi$, and 3π this relative error is approximately 9, 5, and 3%, respectively, when $\xi = 0.5$. Although these relative errors may not seem significant, as ξ approaches one their magnitude

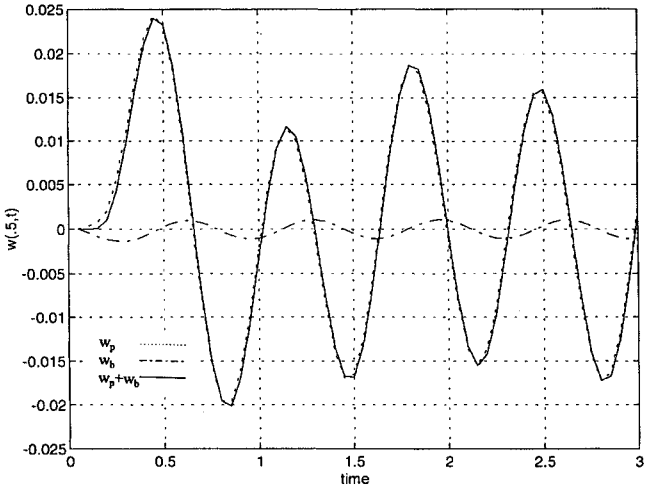

Fig. 7 Time-domain plot of the displacement at $\xi = 0.5$ for a high excitation frequency, $\omega_0 = 3\pi$, comparing the poles-only response, the branch-cut-only response, and the total response.

grows. For example, when $\xi = 0.9$ and the excitation frequency ranges from 1 to 10 Hz, the relative errors range from 25 to 20%. Again this mirrors the behavior seen in Fig. 4.

Conclusions

We have examined a distributed model of a coupon with a fractional-derivative constitutive law. This constitutive relation was chosen to better model the material behavior over a broad frequency range. We found for this coupon model that a forced excitation had an equivalent displacement excitation as given, through the Laplace transform, by Eq. (14). In studying the displacement problem, we separated the transfer function into two parts: that which was associated with the poles of Eq. (17), and that which was associated with the branch-cut integral of Eq. (24).

Each pole and its complex conjugate represent both a left and a right dissipative propagating wave within the material. The strength of dissipation is highly dependent on both the mode number k and the strength of the material's memory as measured by α. This can be seen in Eq. (22) for large k. As the memory in the material diminishes ($\alpha \to 1$), the damping coefficient γ_k increases while the damped natural frequency Γ_k diminishes for each mode. At the other end, as the memory in the material increases ($\alpha \to 0$), the damping coefficient decreases.

The branch-cut integral captures the relaxation behavior of the material. It is found to decay algebraically, as seen from Eq. (26). Its most significant influence takes place near the excitation end

($\xi = 1$) and at frequencies below the first damped natural frequency Γ_k. This agrees with the expected behavior; that is, the relaxation behavior of the material occurs on a much longer time scale than the elastic behavior. The strength of the material's memory also influences the relaxation behavior associated with this branch cut. From Eq. (26) we see that as the memory diminishes ($\alpha \to 1$) the strength of the long-time behavior of the branch cut diminishes. A similar observation is made for the material with perfect memory ($\alpha = 0$). This is consistent with the fact that the branch cut is not necessary for integer-order operators.

The objective is to model materials used in tire manufacture with a constitutive relation that characterizes the material behavior over a broad frequency band. The fractional-derivative Kelvin–Voigt model provided the best fit to the data. However, it also has the complication of introducing the branch-cut integral, for which no closed-form evaluation is in general available. But the majority of the material response can be modeled by the poles-only transfer function h_p in Eq. (19) when the forcing frequency is sufficiently high. This alleviates the need to evaluate that integral.

Acknowledgments

The first and the third author acknowledge the contributions of Air Force Office of Scientific Research, and the second author acknowledges support through the National Research Council. In addition, we would like to thank Arnold H. Mayer of the Wright Laboratory Flight Dynamics Directorate for his assistance and support.

References

[1]Bagley, R. L., and Torvik, P. J., "On the Fractional Calculus Model of Viscoelastic Behavior," *Journal of Rheology*, Vol. 30, No. 1, 1986, pp. 133–155.

[2]Bagley, R. L., and Torvik, P. J., "Fractional Calculus in the Transient Analysis of Viscoelastically Damped Structures," *AIAA Journal*, Vol. 23, No. 3, 1985, pp. 201–210.

[3]Eldred, L. B., Baker, W. P., and Palazotto, A. N., "Kelvin–Voigt Versus a Fractional Derivative Model as Constitutive Relations for Viscoelastic Materials," *AIAA Journal*, Vol. 33, No. 3, 1995, pp. 547–550.

[4]Oldham, K. B., and Spanier, J., *The Fractional Calculus*, Academic, San Diego, CA, 1974.

[5]Koeller, R. C., "Application of Fractional Calculus to the Theory of Viscoelasticity," *Journal of Applied Mechanics*, Vol. 51, June 1984, pp. 299–307.

[6]Padovan, J., Chung, S., and Guo, Y. H., "Asymptotic Steady State Behavior of Fractionally Damped Systems," *Journal of the Franklin Institute*, Vol. 324, No. 3, 1987, pp. 491–511.

[7]Padovan, J., and Guo, Y. H., "General Response of Viscoelastic Systems Modelled by Fractional Operators," *Journal of the Franklin Institute*, Vol. 325, No. 2, 1988, pp. 247–275

[8]Flügge, W., *Viscoelasticity*, 2nd ed., Springer–Verlag, New York, 1975, p. 121.

[9]Zauderer, E., *Partial Differential Equations of Applied Mathematics*, Wiley, New York, 1983, p. 240.

[10]Churchill, R. V., and Brown, J. W., *Complex Variables and Applications*, 5th ed., McGraw–Hill, 1990, p. 169.

[11]Olver, F. W. J., *Asymptotics and Special Functions*, Academic, New York, 1974, p. 112.